

## 147 – Correlative morphological, elemental and chemical analyses of actinide-bearing particles for nuclear safeguards and nuclear forensics

Fabien Pointurier, CEA, DAM, DIF; F-91297 Arpajon, France

### Introduction

The analytical chemistry unit of the Division of Military Applications (DAM) of the French Atomic Energy Commission (CEA) has capabilities for characterizing micrometric particles (so-called particle analysis). These capacities are regularly implemented in support of the IAEA's safeguards. Indeed, the unit is a member of the Network of Analytical Laboratories (NWAL) which carry out bulk and particle analyses of environmental samples (i.e. cotton wipers used to collect dust particles into nuclear facilities by wiping smooth surfaces). Moreover, these capacities are also used in the framework of nuclear forensics, as a complement to "bulk" methods, which involve a dissolution step, lengthy radiochemical treatment and measurement by radiometric ( $\alpha$ -spectrometry) and/or mass spectrometry (ICPMS, TIMS) techniques. Implementation of more direct particle analysis, without or with very short sample preparation, allow reporting results within a shorter analytical delay (24 hours to a few days) than bulk methods and possibly identifying and characterizing components of a mixture.

Several micro-analytical techniques are used for both programs at CEA/DAM. A Large Geometry – Secondary Ion Mass Spectrometer (LG-SIMS) is operational since 2022 for measurement of the isotope composition of individual micro-particles made of actinides (uranium and/or plutonium). The isotope composition is complemented by a morphological description of the particles (size, geometry, surface texture, etc.) thanks to electronic imaging performed with a Scanning Electron Microscope (SEM), by the identification of the other major or minor elements which compose the micro-particles thanks to an Energy Dispersive X-ray Spectrometer (EDS) attached to the SEM, and by the determination of the chemical phase(s) (molecular composition, crystalline structure) of the actinide compounds by means of a micro-Raman spectrometer [1-3]. Furthermore, morphological, elemental and chemical phase analyses can be carried out exactly at the same micrometric spot, i.e. for the same micro-particle, thanks to a coupling device which allows performing the Raman analysis within the SEM measurement chamber (so-called in-SEM Raman spectrometry) [4,5].

The aim of this publication is to describe the SEM/EDS – Raman spectrometer coupling and its application to the correlative morphological, elemental and chemical analyses of actinide-bearing micro-particles. Advantages and limitations of the coupling are discussed and two relevant examples of application to nuclear safeguards and nuclear forensics are presented.

### Materials and methods

Micro-particles are sampled by means of cotton wipers or sticky carbon tapes (electrically conductive adhesives, Agar, Oxford Instruments) fixed on a specimen aluminum stub. The sticky medium is a carbon black-filled acrylic adhesive (poly(methyl methacrylate), or PMMA). The particles are also collected by means of the cotton wipers and deposited onto 1-inch graphite disks (Schunk, Japan) by means of a so-called vacuum impactor device. The graphite disks are covered by a polyisobutyl (PIB) - nonane layer to ensure adhesion of the particles.

The micro-Raman spectrometer ("InVia", Renishaw, UK) is equipped with two lasers with wavelengths of 514 nm (visible, 50 mW) and 785 nm (near-IR, 300 mW), an optical microscope with several

objectives (5×, 20×, 50× and 100×), two gratings (1200 and 1800 l/mm) and a charge-coupled device (CCD) detector. The analyzed area is  $\sim 1 \mu\text{m}^2$  with the visible laser and  $\sim 2\text{--}3 \mu\text{m}^2$  for the near-IR laser. The SEM used in this study (Quanta 200, FEI, the Netherlands) is equipped with a secondary electron (SE) detector, a backscattered electron (BSE) detector, an EDX analyzer (SiLi 30 mm<sup>2</sup> detector, Octane-Plus A, EDAX), and software for automated detection and localization of particles whose average atomic number is above a given threshold (usually 15–20).

In-SEM Raman analyses are carried out thanks to a coupling device called “SEM-SCA” (Renishaw, UK) attached to the SEM (see photography in figure 1). In brief, the laser beams are transferred inside the SEM measurement chamber through mono-mode optical fibers inserted inside a retractable arm, inserted between the BSE detector and the SEM sample holder and is positioned just ahead of the sample (see figure 1). As a consequence, the working distance between the sample and the electronic column must be increased from 10 to  $\sim 20$  mm.

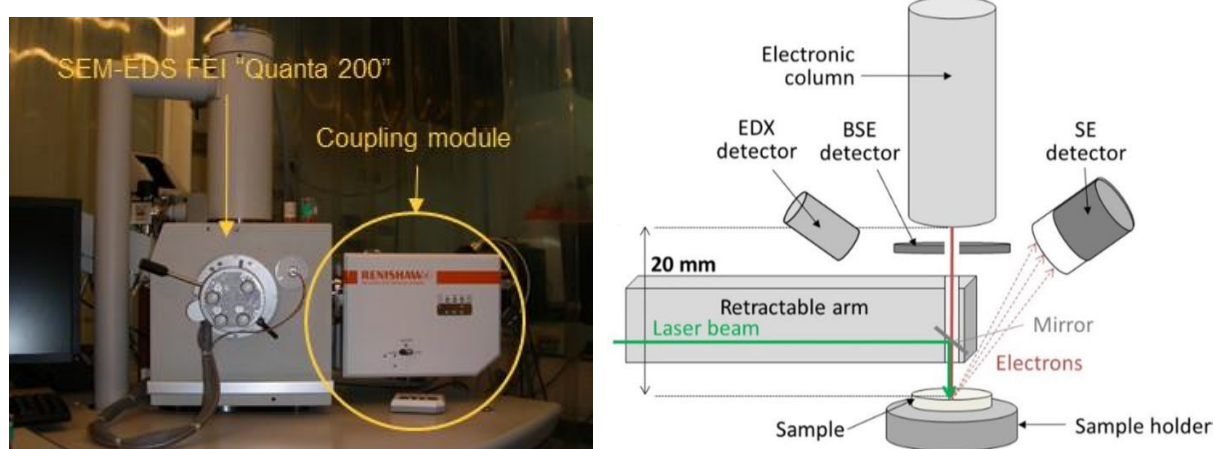


**Figure 1.** Left: photography of the coupling module (SEM-SCA) between a SEM (FEI Quanta 200) and the micro-Raman spectrometer. Right: simplified diagrams of the SEM/EDX when configured for analysis by in-SEM Raman spectrometry.

Analysis by in-SEM Raman spectrometry is not straightforward, as the instrumentation has a few technical limitations. The main ones are the following:

1. When the arm that contains the optical fibers and the mirror is inserted, the EDX detector and the BSE detector can no longer be used. The samples can only be observed with the SE detector.
2. The optical image of the sample, transmitted through a mirror at the extremity of the arm, is very narrow and of poor quality (lack of contrast). Consequently, very small particles ( $\sim 1\text{--}2 \mu\text{m}$ ) may be difficult to relocate in some cases.
3. Once the distance between the bottom of the electronic column and the sample holder is increased and the retractable arm is inserted, each particle of interest is firstly relocated thanks to the electronic image and the sample holder is moved so that the particle is approximately at the center of the electronic image. Similarly, the particle must be exactly at the center of the optical image, so that the laser beam can be properly focused on the particle. However, there is a variable and significant shift (typically a few  $\mu\text{m}$ , up to  $\sim 50 \mu\text{m}$ ) between the electronic and optical images. Therefore, this shift must as precisely as possible be corrected using landmarks that are easily observable on both images (for instance a TEM grid stuck on the edge of the disk).
4. There is a very significant loss of power and consequently of Raman intensity (roughly by a factor of 1 000) with respect to the stand-alone micro-Raman spectrometer, due to losses of light during

transfers through optical fibers in both directions and within the SEM-SCA module. This loss of power can be compensated as only a small fraction of the maximal laser power (50 mW visible laser, 200 mW NIR laser) is applied to the particles. Indeed, the incident power is limited to  $\sim 1$  mW to ensure the conservation of the chemical phase. However, it is much more difficult in the case of in-SEM Raman analysis to find the right balance between an insufficient power supply, which does not provide enough Raman intensity for micrometric objects, and an excessive power which may lead to phase change or thermal decomposition of the particle.

Besides, we observed that overly long and intense electronic scanning degrades the structure of the micro-particles and thereby weakens the Raman scattering intensity. Long electronic scanning may also strongly increase the Raman background, possibly because of the decomposition of the glue (PIB-nonane or PMMA) into degradation products which fluoresces. Therefore, we developed a robust methodology for combined morphological, elemental and chemical analyses by means of SEM/EDS and micro-Raman spectrometry coupling (see figure 2) [6]. Key points of this methodology are: i) location of the particles of interest must be carried out with an as low as possible electron scanning; ii) high resolution electron images and EDX spectra must be carried out after the in-SEM Raman analysis. The duration of the irradiation is generally 10 min ( $10 \times 60$  s) but can be increased if necessary for the smallest analyzable particles (diameters of  $\sim 1$   $\mu\text{m}$ ).

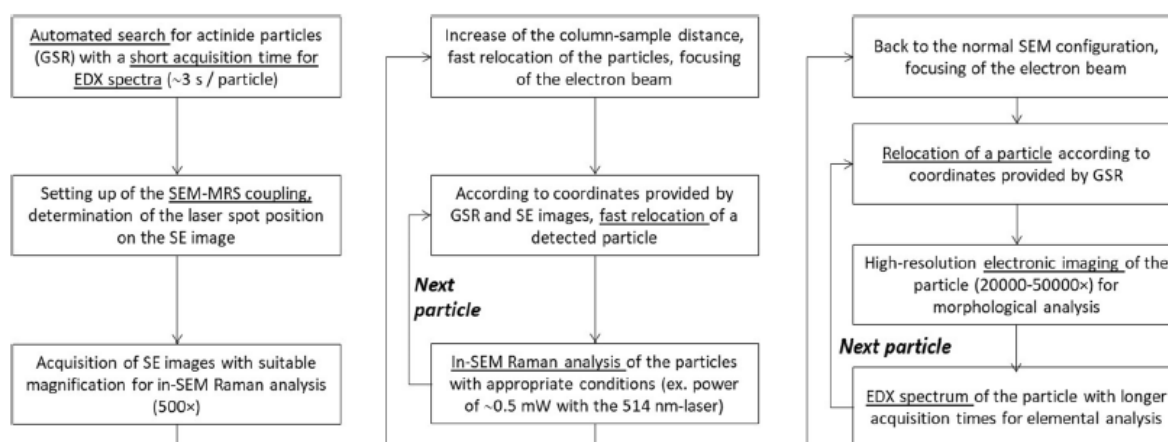


**Figure 2.** Diagram of the recommended analytical procedure for combined morphological, elemental and chemical analyses of micro-particles.

## Results and Discussion

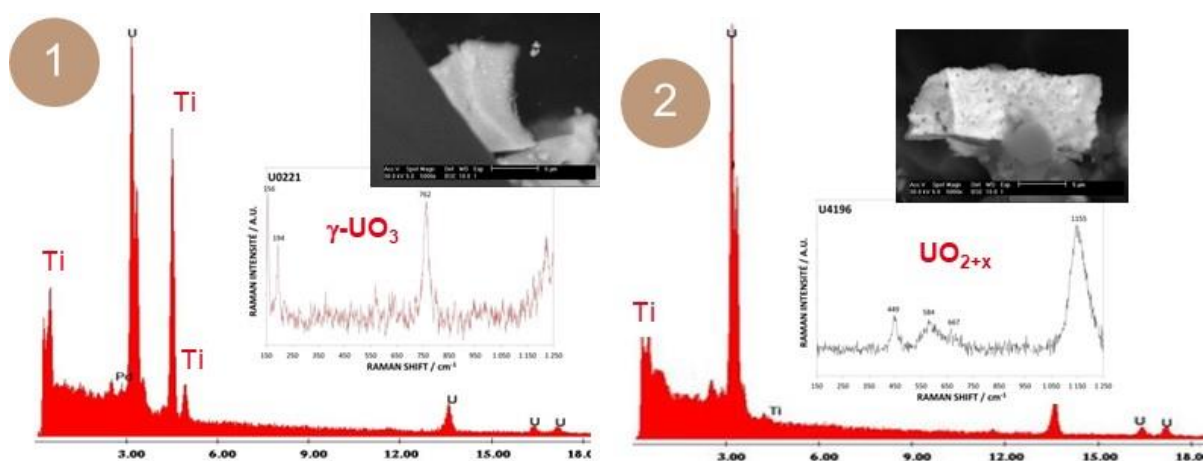
Two examples of correlative analyses by means of the coupling device between the SEM/EDS and the Raman spectrometer are described below. The first analyzed sample called 17/F/38 is dust collected within a fume hood inside a nuclear facility into which nuclear materials are regularly processed. The second sample is a yellow powder referred to as ES-3 from the 7<sup>th</sup> Collaborative Material Exercise organized by the ITWG-NF (International Technical Working Group on Nuclear Forensics).

In the case of the sample 17/F/38, the actinide-bearing particles were scarce with respect to environmental (organic, mineral particles) and non-nuclear anthropogenic particles (lead, iron, etc.). Therefore, the full analytical procedure described above was applied, including the automated search for particles (GSR) to detect and locate specifically the actinide-bearing particles. A few hundreds of U and Th-bearing particles were detected and localized, with sizes ranging from  $\sim 2$   $\mu\text{m}$  to a few tens of  $\mu\text{m}$ . 26 particles were fully characterized by SEM/EDS and in-SEM Raman spectrometry. Five categories of particles with specific and distinctive chemical phases, elemental impurities and morphologies were

evidenced. These particles were produced by different processes implemented in the facility. The results are summarized in Table 1. Typical electronic images, EDX spectra and Raman spectra for each category of particles are given in figure 3. This sample was relatively easy to process as it contains many particles with a sufficient size for in-Raman analysis, i.e., with diameters above  $\sim 5 \mu\text{m}$ . For such analyses, in-SEM Raman spectra are of sufficient quality for identification of the chemical phases. However, it should be mentioned that most of the so-called environmental samples often contain only a few micrometric and mainly sub-micrometric particles. For such samples, recognition of the particles of interest on the optical image – and consequently laser focusing on the particles – proves to be tedious and time-consuming. Besides, the corresponding Raman spectra generally show poor signal-to-noise ratios and identification of the chemical phases may be impossible for a significant fraction of the analyzed particles.

**Table 1.** Results of the correlative morphological, elemental and chemical analysis by SEM/EDS and in-SEM Raman spectrometry for the sample 17/F/38. The detected minor elemental constituents, if any, are within parentheses. (-) means that no minor constituent was detected.

Category number	Number of analyzed particles	Chemical phase	Main elemental constituents: major (and minor)	Short morphological description
1	6	UO <sub>3</sub>	U, O (Ti)	Blocky, sharp edges, smooth surfaces
2	3	UO <sub>2</sub>	U, O (Ti)	Blocky, sharp edges, porosities
3	3	UO <sub>3</sub> ·x(H <sub>2</sub> O)	U, O (Cl)	Blocky, rounded edges, porosities
4	11	U <sub>4</sub> O <sub>9</sub>	U, O (Ti)	Agglomerates, rounded sub-particles
5	3	ThO <sub>2</sub>	Th, O (-)	Agglomerates, tip-shape sub-particles



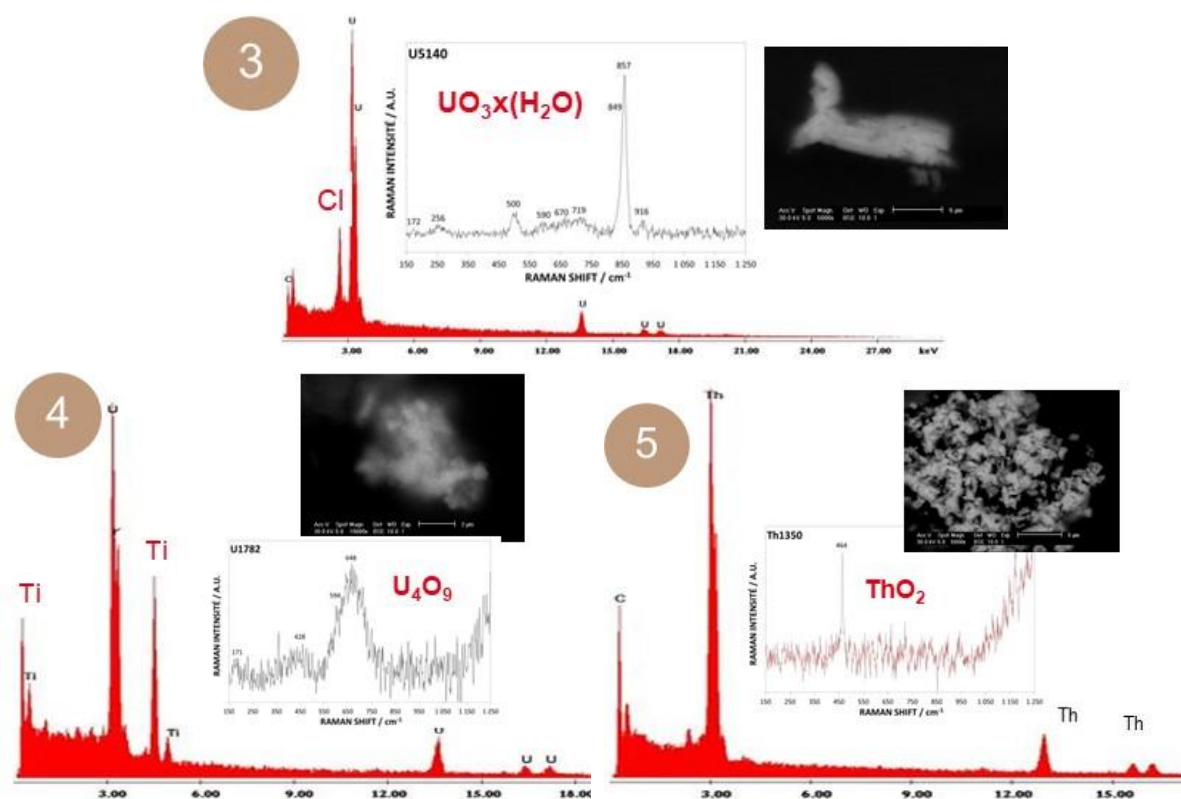


**Figure 3.** Typical examples of electronic images, EDS spectra, and in-SEM Raman spectra for one particle of each category of actinide-bearing particles detected in the sample 17/F/38.

By contrast, the sample ES-3 consisted only of uranium-bearing particles sampled by means of a sticky carbon tape. As numerous uranium particles were present on the disk and easily detected by electronic imaging, no automated detection of particles was carried out. 11 uranium particles were randomly selected for correlative morphological, elemental and chemical analysis by SEM/EDS and in-SEM Raman spectrometry. Two categories of particles with specific chemical phases, elemental impurities and morphologies were evidenced, showing that this powdered sample can be regarded as a mixture of two different compounds. The results are summarized in [Table 2](#). Typical electronic images, EDX spectra and Raman spectra for each category of particles are given in [figure 4](#). Firstly, two distinct morphologies are observed. The lexicon proposed by Tamasi et al. [7] was considered for establishing the morphological description. In brief, the first morphology (category 1, 5 particles out of 11) consists of individual sub-rounded blocky particles with smooth surfaces and often with cracks and/or a molten aspect. The Raman spectra of these particles closely match the one of uranyl nitrate  $\text{UO}_2(\text{NO}_3)_2$  (mainly a strong peak at  $\sim 870 \text{ cm}^{-1}$  in the uranyl region and a medium intensity peak at  $\sim 1040 \text{ cm}^{-1}$  assigned to nitrate ionic species). No other chemical element than U, N and O were detected by EDS. The second morphology (category 2, 6 particles out of 11) consists of agglomerates of flat and smooth pin-shaped and radially distributed sub-particles. The Raman spectra of these particles are in agreement with the spectrum of uranyl oxohydroxide  $(\text{UO}_2)_8\text{O}_2(\text{OH})_{12}\cdot 12(\text{H}_2\text{O})$  (major intense peak at  $\sim 840 \text{ cm}^{-1}$ ) or *schoepite*. Besides, Ca was detected as a minor constituent in all of these particles. Indeed, the K-line of Ca is clearly detected at 3.69 KeV in all of these EDS spectra, whereas it is hardly or not at all observed in the EDS spectra of particles of the first category. It is impossible to determine if these two compounds were originally present in the powdered sample ES-3 or if one of the compounds is a degradation product of the other one. The most likely hypothesis is a phase change from uranyl nitrate to uranyl oxy-hydroxide, possibly promoted by presence of Ca.



**Table 2.** Results of the correlative morphological, elemental and chemical analysis by SEM/EDS and in-SEM Raman spectrometry for the sample ES-3. The detected minor elemental constituents, if any, are within parentheses. (-) means that no minor constituent was detected.

Category number	Number of analyzed particles	Chemical phase	Main elemental constituents: major (and minor)	Short morphological description
1	5	$\text{UO}_2(\text{NO}_3)_2$	U, O, N (-)	Rounded-blocky, smooth surfaces
2	6	$(\text{UO}_2)_8\text{O}_2(\text{OH})_{12}\cdot 12(\text{H}_2\text{O})$	U, O (Ca)	Radial pin-shape agglomerates

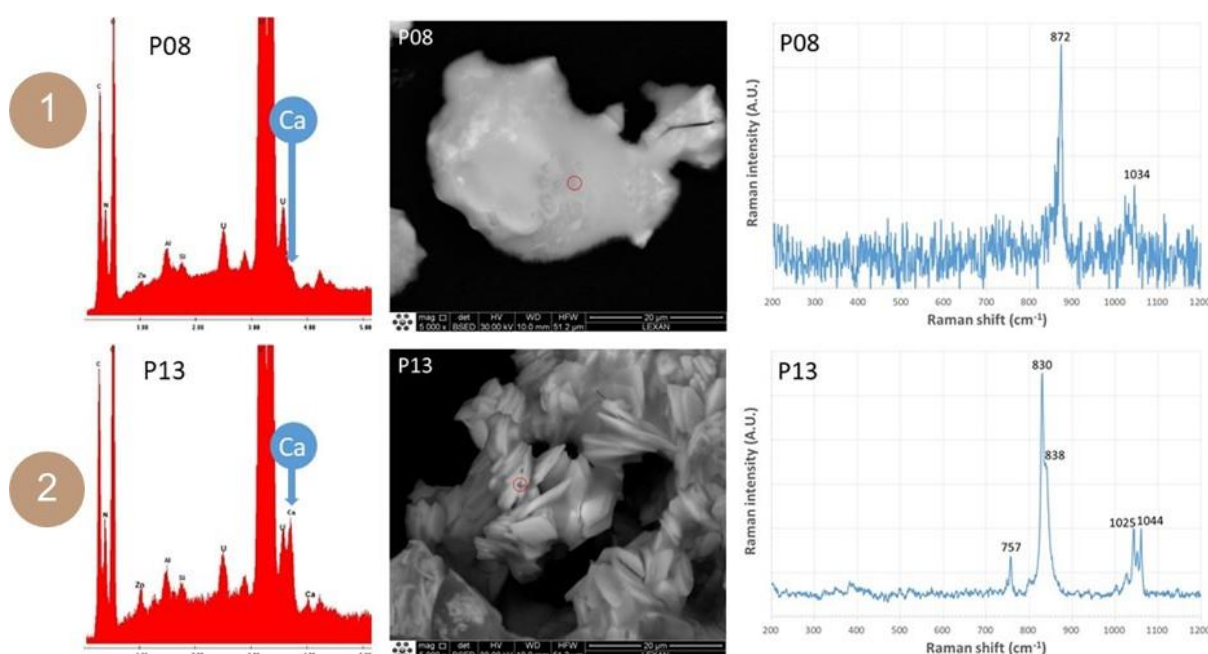


**Figure 4.** Typical examples of electronic images, EDS spectra, and in-SEM Raman spectra for one particle of the two categories of actinide-bearing particles evidenced in the sample ES-3.

## Conclusion and Perspectives

Despite a few technical limitations, the combination of SEM/EDS and in-SEM Raman analyses thanks to an original coupling device between the two instruments provides morphological, elemental and chemical expertise at the scale of individual micro-particles. Such correlative analyses may be of potential interest in many fields. We presented here two relevant examples of correlative analyses in nuclear safeguards and nuclear forensics. This coupling device may also be of great interest for other applications, like characterization of particles candidate for particulate reference materials, especially mixed oxide particles, for instance U-Th oxide or U-Ce oxide particles. In such cases, correlative analyses may be useful to study internal and between particles elemental homogeneity, and to link possible heterogeneity with morphology and/or phase changes.

## References

- [1] F. Pointurier, O. Marie, *Spectrochim. Acta B* **65** (2010) 797–804.
- [2] F. Pointurier, D.M.L. Ho, D. Manara, O. Marie, T. Fanghänel, K. Mayer, *Vib. Spec.* **103** (2019) 102925.
- [3] F. Pointurier, C. Lelong, O. Marie, *Vib. Spec.* **110** (2020) 103145
- [4] F. Pointurier, O. Marie, *J. Raman Spectrosc.* **44** (2013) 1753–1759.
- [5] E.A. Stefaniak, F Pointurier, O. Marie, J. Truyen, Y. Aregbe, *Analyst* **139** (2014) 668-675.
- [6] F. Pointurier, O. Marie, *J. Radional. Nucl. Chem.* (2023) <https://doi.org/10.1007/s10967-022-08712-4>
- [7] A.L. Tamasi, L.J. Cash, C. Eley, R.B. Porter, D.L. Pugmire, A.R. Ross, C.E. Ruggiero, L. Tandon, G.L. Wagner, J.R. Walensky, A.D. Wall, M.P. Wilkerson., *J. Radioanal. Nucl. Chem.* **307** (2016) 1611-1619.